Shahrood University of Technology

Journal of Hydraulic and Water Engineering (JHWE)

Journal homepage: https://jhwe.shahroodut.ac.ir

Iranian Hydraulic Association (IHA)

Experimental Evaluation of Mechanical Properties of Alkali-Activated Blast Furnace Slag Concrete vs. Portland Cement in Hydraulic Structures

Mohammadhossein Mansourghanaei [1,*]

[1]Ph.D. in Civil Engineering, Department of Civil Engineering, Chalous Branch, Islamic Azad University, Chalous, Iran.

Article Info

Article History:

Received 21 March 2025
Received in revised form 8 December 2025
Accepted 14 June 2026
Published online 18 June 2026

DOI:10.22044/jhwe.2026.15958.1056

Keywords

Hydraulic Structures
Ordinary Portland Cement Concrete
Alkali-Activated Concrete
Compressive Strength
Tensile Strength

Abstract

Improving the mechanical properties and durability of concrete used in hydraulic structures has always been of interest to civil engineers. In this paper, the mechanical properties of alkali-activated concrete (AAC) were evaluated compared to ordinary portland cement concrete (OPCC) for use in hydraulic structures. In this research paper, a mix design of OPCC containing 500 kg/m^3 of Portland cement and a mix design of AAC containing granulated blast furnace slag (GBFS) were made. The mechanical properties of the designs were evaluated under compressive strength, tensile strength and elastic modulus tests at 7, 28 and 90 days of curing. The test results indicate that the performance improves with increasing curing age in concrete samples. In this regard, in OPCC, the highest compressive strength, tensile strength and elastic modulus were obtained at 90 days of curing age, respectively, with values of 64.92, 5.22 MPa and 33.73 GPa, which achieved 48.79, 89.13 and 21.85 percent improvement in results compared to 7 days of curing age. In AAC, the highest compressive strength, tensile strength and elastic modulus were obtained at the 90-day curing age, which were 72.33, 4.74 MPa and 39.11 GPa, respectively, which resulted in 10.93, 60.67 and 25.35 percent improvement in results compared to the 7-day curing age. At the 90-day curing age (as the optimal age), the performance of AAC in compressive strength, tensile strength and elastic modulus tests showed 11.41% improvement, 19.9% decrease and 15.95% improvement in results, respectively. The results obtained from scanning electron microscopy (SEM) analysis on concrete samples overlapped with other tests in this study.

1. Introduction

Many concrete hydraulic structures are built around the world every year. In this regard, a large volume of concrete is produced and used as the main material for hydraulic structures. Therefore, the selection of concrete type and concrete materials will greatly help in improving the mechanical properties and durability of hardened concrete. In this regard, due to the low properties of OPCC, scientists have developed alternative concretes for use in concrete hydraulic structures. On the other hand, OPCC production has always been associated with disadvantages such as low strength of the resulting concrete and environmental pollution due to the emission of toxic carbon dioxide gas (as a result of the cement production process). Research shows that cement factories are responsible for the emission of about 5% of the total carbon dioxide entering the Earth’s atmosphere (Nosrati et al., 2018). In order to solve these problems, civil engineering researchers were

* *Corresponding Author:* Mhm.Ghanaei@Gmail.Com, Tel:+989121712070

thinking of finding an alternative material to cement in concrete. They introduced fly ash, metakaolin, GBFS and other pozzolans as suitable cement substitutes (Nuaklong ei al., 2016: Singh et al., 2015: Zhuang et al., 2016). GBFS, as an artificial pozzolan, is a by-product of iron smelting plants. It has been reported that, for every ton of steel produced, 300 kg to one ton of GBFS is obtained, which shows the importance of using these secondary products in various industries. On the other hand, studies have shown that concretes containing GBFS have greater resistance to sulfate attack (Ganesh et al., 2016: [1]Mansourghanaei et al., 2024: [2]Mansourghanaei et al., 2024: [3]Mansourghanaei et al., 2023: [4]Mansourghanaei and Mardookhpour, 2024: [5]Mansourghanaei et al., 2023). Replacing the entire cement consumed in concrete with GBFS leads to the production of AAC. If the aluminosilicate materials present in the cement replacement materials have the highest volume, this type of concrete is called geopolymer concrete. The aluminosilicate network is composed of SiO_4 and AlO_4, tetrahedral structural units that can be connected to each other and share their oxygen atoms (Allahverdi et al., 2011). Davidowitz (Davidovits, 2008) defined the chemical structure of geopolymers in 1972. The amount of carbon dioxide produced in the geopolymerization process is much lower than that of ordinary cement production (Neupane et al., 2018). The production of AAC is carried out by OPCC technology methods (Vora and Urmil, 2013). By adding slag to the concrete mixture, the pore structure in the concrete is optimized and the pore size distribution is more appropriate, the interfacial transition zone (ITZ) is denser, and the strength and durability aspects of the concrete are gradually increased. In other words, the development of strength and durability is closely related to the evolution of the pore structure and ITZ in alkali-activated slag concrete (AASC) (Duan et al., 2013). The mechanical properties of concrete are affected by various factors such as the type, amount, and characteristics of the materials used. In this regard, in concretes with a low water-to-cement ratio, the appropriate amount of cement causes a higher concentration of the cement paste and a reduction in the space for the available water, which results in the cement particles approaching each other, after the hydration or polymerization process and geopolymerization, the pores of the concrete become smaller and these small pores are also blocked due to the continuation of the chemical reaction (Naderi et al., 2018). Research has shown that the grade of cement used in the concrete composition has a direct effect on its elastic modulus (Kazemian and Ghareh, 2017). On the other hand, the method and age of curing in concrete can have an effective role in the mechanical properties of concrete. In this regard, research has shown that the rate of acquisition of compressive strength and elastic modulus of concrete increases rapidly at early ages ([1]Mansourghanaei et al., 2024: [4]Mansourghanaei and Mardookhpour, 2024: Abd Elaty, 2014: Kim et al., 1998: Madandoust et al., 2012: Pirmohammadi Alishah and Mahmoudzadeh, 2020). Dissolution of cementitious materials in OPCC is carried out by calcium hydroxide known as portlandite ($Ca(OH)_2$). However, in AAC, activation of GBFS with alkali-activated solution (AAS) such as sodium hydroxide (NaOH) and sodium silicate (Na_2SiO_3) to produce AASC has been studied in the past few decades (Duan et al., 2013). In this regard, studies have shown that the combined use of NaOH and Na_2SiO_3, due to the formation of larger amounts of hydrated calcium silicate gel (C-S-H) when using calcium silicate, leads to higher compressive strength than the case of using $Ca(OH)_2$ alone (Shirgir et al., 2017).

In general, hydraulic structures are very important for sustainable management of water resources, but diverting the river course to build hydraulic structures can lead to problems such as environmental issues, so awareness of hydraulic conditions is very important (Jorabloo et al., 2024: Khalighi et al., 2024). Another important point in dam design is hydrostatic pressures, which can affect the dam structure in various ways. Hydrostatic pressure can penetrate cracks and gaps in the dam body, causing the dam to fail (Hatami Zargaran, 2024).

The objectives and innovations in this experimental research through the production of AAC can be summarized as follows:

1- The mechanical and microstructural properties of AAC are improved compared to OPCC.

2- Helping to reduce the volume of toxic carbon dioxide emissions compared to OPCC production, according to the report provided by other researchers in this regard.

3- Helping to maintain environmental health by using (in the composition of AAC) slag accumulated in iron smelting plants, known as environmentally harmful materials.

4- Conserving and reducing the consumption of consumable mineral resources that are used as main materials during the ordinary cement manufacturing process.

5- Conserving and reducing the consumption of fossil fuels that are used as fuel in ordinary cement production plants.

2. Matrials and Methods

In this experimental study, Portland cement type 2, produced by Gilan Sabz Cement Industries (Dilman), with a density of 3250 kg/m^3 and a specific surface area of 3000 to 3200 cm^2/g, which was produced under the ISIRI 389 standard, was used. GBFS from the blast furnace, produced by the Isfahan Iron and Steel Plant, with a density of 2750 kg/m^3, a specific surface area of 2200 cm^2/g, and a bulk density of 960 kg/m^3, was used under the ASTM C989/C989M standard. The chemical characteristics of GBFS and Portland cement are shown in Table 1. The water used to prepare lime water and make the mixture design in the present study was from the drinking water of Lahijan city. This water has a pH in the range of 6.5 to 7.5 and a density of 1000 kg/m^3. According to Section 2-4-10-9 and 3-4-10-9 of the Fourth Edition of the National Building Regulations of Iran, water that is potable, has no distinct taste or odor, and is clean and clear can be used in concrete without testing, unless previous records indicate that this water is unsuitable for concrete. The aggregate used is synthetic and based on the requirements of the ASTM C33 standard, obtained from sand and gravel factories in Lahijan city. Some of the characteristics of the aggregate used are shown in Table 2. Research has shown that fresh AAC has poorer performance due to the high viscosity of the AAS compared to fresh OPCC. To solve this problem, a polycarboxylate normal superplasticizer (PCNS) is often the best option due to the strong bonds between positively charged calcium and negatively charged polycarboxylate (Pilehvar et al., 2018). In this regard, a fourth-generation superplasticizer based on normal polycarboxylate, a product of Durochem Middle East Company, was used based on the characteristics in Table 3. The AAS used in this study is a combination of Na_2SiO_3 and NaOH solution with a weight ratio of 2.5, which was used with a combined density of 1483 kg/m^3. Some of the characteristics of the AAS used in this study are shown in Table 4. Figure 1 shows concrete samples subjected to compressive strength, tensile strength, and modulus of elasticity tests.

2.1. Mix Design

There is no separate standard for the design of AAC mix, therefore, in this study, following some experimental studies (Ganesh et al., 2016: [1]Mansourghanaei et al., 2024: [2]Mansourghanaei et al., 2024: [3]Mansourghanaei et al., 2023: [4]Mansourghanaei and Mardookhpour, 2024: [5]Mansourghanaei et al., 2023: Deb et al., 2015), the design of AAC mix was prepared and adjusted in accordance with the standard for the preparation of OPCC under the recommendation of the ACI Committee 211.1-89 based on Table 5.

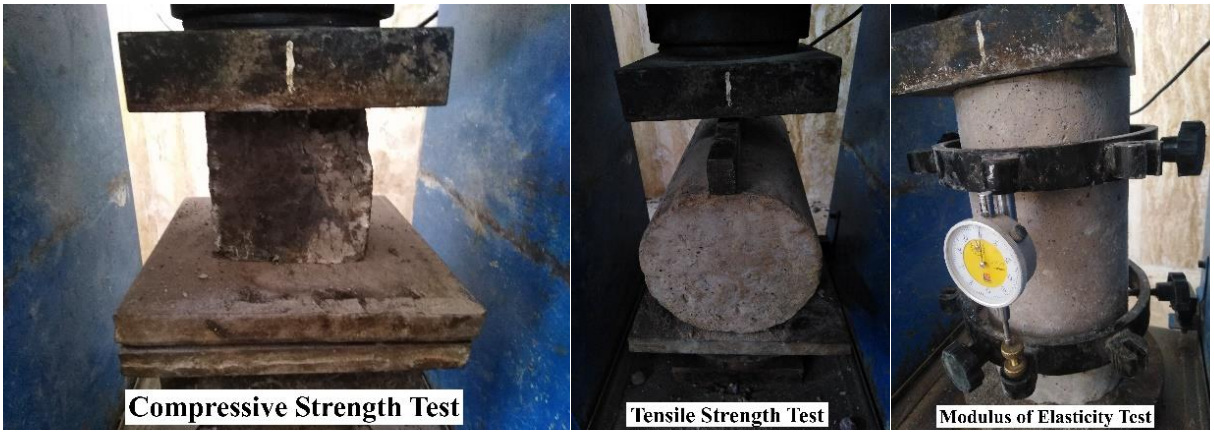

Figure 1. Concrete Samples Under Test

Table 1. Chemical Characteristics of GBFS and Portland Cement (%)

Component	SiO_2	Al_2O_3	Fe_2O_3	CaO	MgO	SO_3	K_2O	Na_2O	TiO_2	LOI
GBFS	29.2	19.4	5.8	38.6	2.8	2.6	0.1	0.2	0.6	0.3
Portland Cement	21.3	4.7	4.3	62.7	2.1	2	0.65	0.18	-	1.84

Table 2. Aggregate Specifications

Concrete Aggregates	Minimum Diameter	Maximum Diameter (mm)	Modulus of Elasticity (mm)	Density (kg/m^3)	Water Absorption (%)
Gravel	4.75 (mm)	19	5.7	2750	2.2
Sand	75 (μm)	4.75	2.85	2650	2.9

Table 3. PCNS Specifications

Chemical Formula	Physical Condition	Color	Density (kg/m^3)	Consumption Standard	pH
Normal Polycarboxylate	Liquid	Light Brown	1100	ASTM C494	About 7

Table 4. AAS Specifications

Formula	Color	Molarity (mol/m^3)	Density (kg/m^3)	Modulus of Elasticity (GPa)	Melting Temperature (C)	Molar Mass (gr/mol)	*	**
NaOH	Colorless	12	2130	3.3	318	39.99	-	-
Na_2SiO_3	Colorless	12	2400	-	1088	122.06	2.4	47

* Molar Weight Ratio of Silicate to Sodium ** Molar Weight Ratio of Silicate to Water

Table 5. Concrete Mix Design Specifications

Concrete Type	Materials / Quantity	Cement	GBFS	Water	Sand	Gravel	PNS*	Density (kg/m^3)	Curing
OPCC	kg/m^3	500	0	225	1000	765	7	2497	Water
	%	20.02	0	9.01	40.04	30.63	0.0028		
AAC	kg/m^3	0	500	225	1000	762.63	7	2494	Heat + dry Environment
	%	0	20.04	9.19	40.08	30.57	0.0028		

* Polycarboxylate Normal Superplasticizer
- Water to cement (W/C) ratio in OPCC and AAC = 45 %
- In AAC, the W/C ratio refers to the ratio of AAS to the GBFS used.

2.2. Construction and Curing

Initially, the materials were weighed according to the mixing plan in Table 5, and then the dry materials including cement (or GBFS) and aggregate were poured into the rotating electric mixer, and the mixing process lasted for 1.5 minutes. Next, the wet materials including water (or AAS) were added to the mixture, and the mixing of the materials lasted for another 2.5 minutes. Then, the fresh concrete mixture was poured into the foil-lined and oiled metal molds in three stages. In this regard, in order to apply compaction, 25 blows were applied to the concrete mixture in each stage by a special rod. Finally, the molds containing the concrete samples were stored in a dry environment at a temperature of 21 ℃. After this time, the samples were demoulded, and the OPCC samples were stored and cured in lime water at a temperature of 21 ℃ until the test age. After molding, the AAC samples were subjected to heat treatment in a furnace at 60 ℃ for 48 hours to improve the strength of this type of concrete. After this time, the concrete samples were removed from the furnace and stored and cured in a dry environment at 21 ℃ until the test time. In terms of heat treatment in AAC, research has shown that AAC samples subjected to heat treatment at 50 to 70 ℃ have higher strength than samples under 20 ℃ ([1]Mansourghanaei et al., 2024: [2]Mansourghanaei et al., 2024: Mehta and Monteiro, 2014).

2.3. Standard and Method of Testing

The compressive strength test of concrete at the age of 7, 28 and 90 days was carried out in accordance with the BS 12390-3 standard on cubic samples with dimensions of 10×10×10 cm. In this regard, the samples were placed in a concrete-breaking jack device in such a way that the two opposite surfaces that were adjacent to the mold during concrete pouring were in contact with the upper and lower stirrups of the device. After the samples were solidified, the force loading was carried out within the standard range at a speed of 0.9 MPa/s (54 MPa/min) in a constant, uniform manner, without sudden changes and perpendicular to the direction of concreting until the moment of concrete sample failure. The maximum applied load determines the amount of resistance of the concrete sample to the applied pressure. Tensile strength tests of concrete at curing ages of 7, 28 and 90 days were performed according to ASTM C496 on cylindrical specimens with dimensions of 30×15 cm. In this regard, the specimens were placed longitudinally under a concrete-breaking jack and the force was applied according to the standard until the concrete specimen broke. The maximum applied load determines the resistance of the concrete specimen to the applied pressure. Modulus-elasticity tests of concrete at curing ages of 7, 28 and 90 days were performed according to ASTM C469 on cylindrical specimens with dimensions of 30×15 cm. In this regard, the desired sample was placed inside the concrete modulus of elasticity test frame, then a concrete sample with a cross section of 15 cm was placed vertically between the two plates of the concrete-breaking jack device, then an applied load was applied at a speed of between 0.5 and 0.9 kN/s until the final deformation of the sample was introduced on its vertical axis, the longitudinal deformation of the concrete sample was measured using a gauge or strain gauge attached to the frame. SEM image analysis was performed at a curing age of 90 days in the cured concrete at a temperature of 21 ℃ using a scanning electron microscope with the FEI Quanta200 model. In this regard, the crushed concrete sample was placed in the device and the images were recorded at the desired magnification and then subjected to microstructural examination.

3. Results and Discussions

3.1. Compressive Strength Test Results and Interpretation

The results of the concrete compressive strength test in this study are shown in Figure 2. Other studies have shown that the strength growth of AAC based on GBFS is very rapid in the early days ([1]Mansourghanaei et al., 2024: [2]Mansourghanaei et al., 2024: [3]Mansourghanaei et al., 2023), such that this type of resistant concrete achieves about 70% of its final compressive strength at the age of 7 days (Nofallah, 2018). In this regard, and based on the results of the graph in Figure 2, it is evident that increasing the curing age of concrete has improved the results in each of the concrete designs. This performance has also been concluded in other studies ([1]Mansourghanaei et al., 2024: [2]Mansourghanaei et al., 2024: [4]Mansourghanaei and Mardookhpour, 2024). In OPCC, the highest compressive strength was achieved at the age of 90 days, at 64.92 MPa, which resulted in an improvement of 48.79% compared to the age of 7 days. In AAC, the highest compressive strength was obtained at a curing age of 90 days, which was 72.33 MPa, which was an improvement of 10.93% compared to the 7-day curing age. At all curing ages, the results of the compressive strength test in AAC were superior to the results of the compressive strength test in OPCC, such that at curing ages of 7, 28, and 90 days, the improvement in compressive strength in AAC compared to OPCC was 49.43, 20.82, and 11.41%, respectively. In this regard, research by Jafari Nadoshan and Ramazanianpour has shown that the 91-day compressive strength of activated alkali cement paste based on GBFS is about 74% higher than that of OPCC (Jafari Nadoushan and Ramezanianpor, 2019). This is due to the high pozzolanic activity of GBFS particles in the composition of AAC. In this regard, the aluminosilicate particles present in the slag, while accelerating the geopolymerization process, have produced a high volume of hydrated gels such as C-S-H, hydrated calcium aluminum silicate known as ettringite (C-A-S-H) and hydrated sodium aluminum silicate known as tobermorite (N-A-S-H), in the AASC matrix. These gels, by filling cracks, cavities, interlayer pores and creating a bond in the ITZ, the interface between the paste and the aggregates, create density and strength in the hardened cement paste.

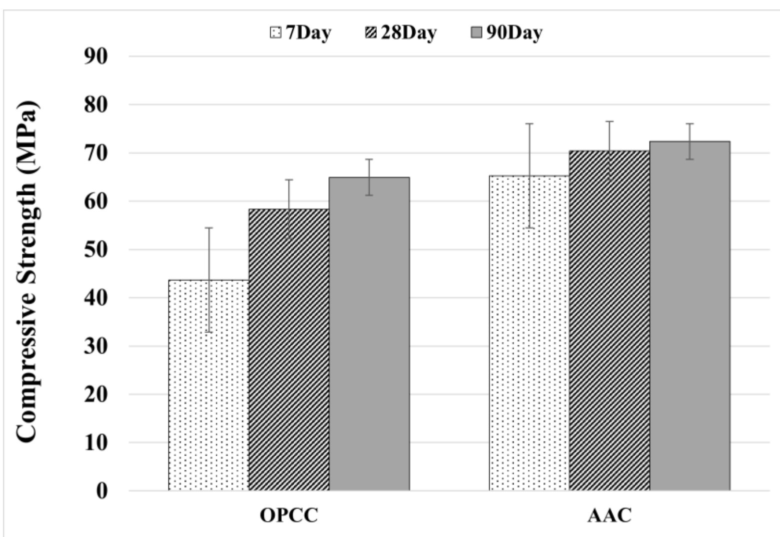

Figure 2. Compressive Strength Test Results

3.2. Results and Interpretation of Tensile Strength Test

The results of the tensile strength test of concrete are presented in accordance with the diagram in Figure 3. According to this diagram, it is evident that increasing the curing age of concrete has improved the tensile strength results. This performance has also been proven in other research (in the field of AAC) ([1]Mansourghanaei et al., 2024: [2]Mansourghanaei et al., 2024: [4]Mansourghanaei and Mardookhpour, 2024:

[5]Mansourghanaei et al., 2023). In this regard, in OPCC, the highest tensile strength was obtained at a curing age of 90 days, which was 22.5 MPa, which resulted in an improvement of 13.89% compared to a curing age of 7 days. In AAC, the highest tensile strength was obtained at a curing age of 90 days, which was 74.4 MPa, which resulted in an improvement of 67.60% compared to a curing age of 7 days. At 7 and 28 days of curing, the tensile strength test results in AAC are 88.6 and 66.8 percent superior to the tensile strength test results in OPCC at the corresponding ages, respectively, but at 90 days of curing, we see a 19.9 percent drop in the tensile strength test results of the AAC sample compared to OPCC. The improvement in the results in AAC compared to OPCC is a result of the production of a high volume of the chemical process product (between the GBFS and the AAS) which are hydrated gels. Hydrated gels play the main role in creating strength in hardened concrete. With increasing curing age in concrete and the progress of the polymerization and geopolymerization process, we will have improved density and strength in concrete.

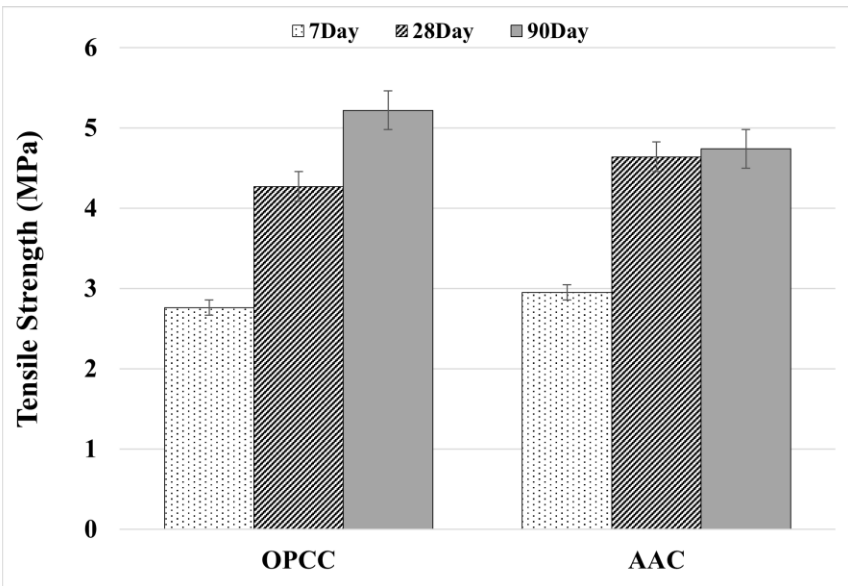

Figure 3. Tensile Strength Test Results

3.3. Results and Interpretation of the Modulus of Elasticity Test

The stress-strain curve of concrete is drawn to investigate the amount of deformation of concrete under uniaxial compressive loading. The behavior of concrete under compressive stress is related to several factors such as concrete strength, loading duration and rate, and properties of the materials used in the concrete mix.

In general, the stress-strain diagram of ordinary unreinforced concrete under uniaxial compressive loading (28 days) is similar to Figure 4. The ultimate strain (ε_u or ε_c) of ordinary concrete against the ultimate strength (f_u or f_c) of the concrete member is in the range of 0.003 to 0.0015, while the rupture strain (ε_R) of concrete is reported to be greater than 0.003. In this curve, it is observed that the behavior of concrete will be almost linear up to 40% of its ultimate strength (f_c), beyond this value, the deformation of concrete will be nonlinear.

The modulus of elasticity of concrete (E_c) is the tangent of the stress-strain curve (relative length change) of concrete, and its value depends on several factors such as the characteristic strength of concrete, loading rate, specifications of the materials used, etc.

The modulus of elasticity of ordinary concrete can be calculated in megapascals (MPa) according to the ACI 318 standard from equation (1). Where fc is the ultimate compressive strength of concrete at 28 days. Figure 5 shows the stress-strain diagram of concrete considering the changes in the modulus of elasticity of concrete (E_c) in the state of ultimate strength (f_c) and rupture strength (f_R) of unreinforced concrete. The initial modulus is the slope of the line to which a tangent curve is drawn from any unspecified point, and the secant modulus is the slope of the line that is connected from the origin to a point on the curve that is equal to 40% of the ultimate stress at rupture.

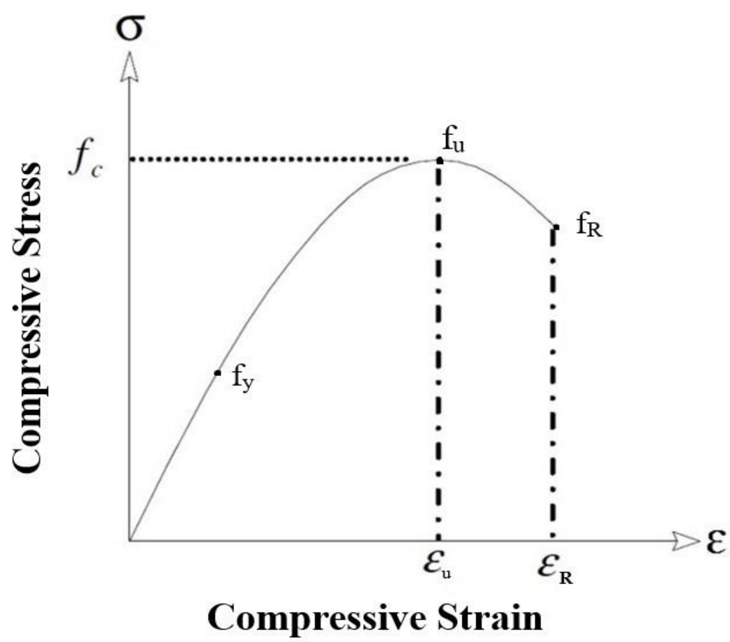

Figure 4. Stress-Strain Curve of Ordinary Unreinforced Concrete in Compression

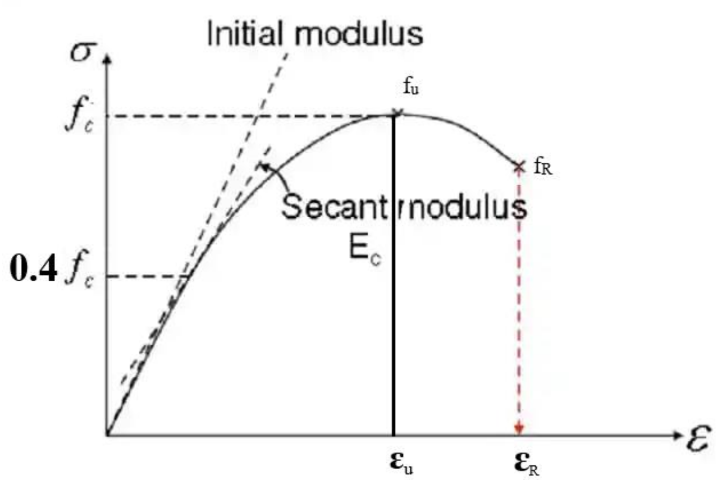

Figure 5. Changes in the Modulus of Elasticity According to the Stress-Strain Curve of Ordinary Unreinforced Concrete in Compression

$$E_c=4700\sqrt{fc} \quad (1)$$

The results of the modulus of elasticity test of concrete in this article are shown in the diagram in Figure 6. According to these results, it is evident that increasing the curing age in concrete samples has improved the results. Similar results have been obtained in the research of others (in the field of AAC) ([2]Mansourghanaei et al., 2024: [4]Mansourghanaei and Mardookhpour, 2024: [5]Mansourghanaei et al., 2023). In this regard, in OPCC, the highest modulus of elasticity was obtained at a curing age of 90 days, which was 33.73 GPa, which resulted in an improvement of 21.85% compared to a curing age of 7 days. In AAC, the highest modulus of elasticity was obtained at a curing age of 90 days, which was 39.11 GPa, which resulted in an improvement of 25.35% compared to a curing age of 7 days. The results of the modulus of elasticity in AAC at the curing age of 7, 28 and 90 days showed an improvement of 12.71, 17.98 and 15.95 percent compared to regular concrete at the corresponding ages, respectively. As the chemical reaction process in concrete progresses with increasing curing age, we see an improvement in the density and strength in the microstructure of the concrete, this is due to the completion of the production of a large part of the volume of hydrated gels in the concrete mixture.

3.4. SEM Results and Interpretation

Images obtained from scanning electron microscopy at a scale of 5 μm on samples of normal concrete and AAC are shown in Figure 7. In the images, a tree structure resulting from the weak volume deficiency of hydrated gels that could not cover the pores well is seen in normal concrete. The volume of hydrated gels (dark colored areas) is much higher in AAC than in normal concrete. Unhydrated particles (small white particles) are more abundant in normal concrete than in AAC due to impurities in the raw materials or the lack of participation of cement particles in the polymerization and geopolymerization process. Pores, pores and microcracks are more abundant in the structure of the paste of normal concrete than in AAC. One of the reasons for the superior compaction in the microstructure of AAC compared to OPCC is the presence of abundant aluminosilicate particles (resulting from the use of GBFS) in the composition of AAC, which, while accelerating the geopolymerization process, has been able to produce a larger volume (according to SEM images) of hydrated gels. These gels, by filling pores, cavities, cracks and bonds in the ITZ, create adhesion and strength in the hardened concrete. In OPCC, in the bulk part of the Portland cement paste, ions such as calcium, sulfate, hydroxide, and aluminate, which are formed through aerobic dissolution into calcium silicate and calcium aluminate, combine to form C-A-S-H and $Ca(OH)_2$ gels, meaning that C-A-S-H is formed as a result of the reaction of calcium aluminate with calcium sulfate, and as the polymerization progresses, weak C-S-H crystals and second-generation crystals formed from $Ca(OH)_2$ and C-A-S-H gel begin to fill the empty spaces in the C-A-S-H and $Ca(OH)_2$ network, and with this operation, the density, hardness, and ITZ strength of the concrete increase (Mehta and Monteiro, 2014). Research by others has shown that in AAC, the pozzolanic reaction, by converting CH to C-S-H, densifies and homogenizes the microstructures (Neupane et al., 2018). In this regard, the effects of superior strength in AAC compared to OPCC are fully evident in the results of compressive strength, tensile strength and elastic modulus tests.

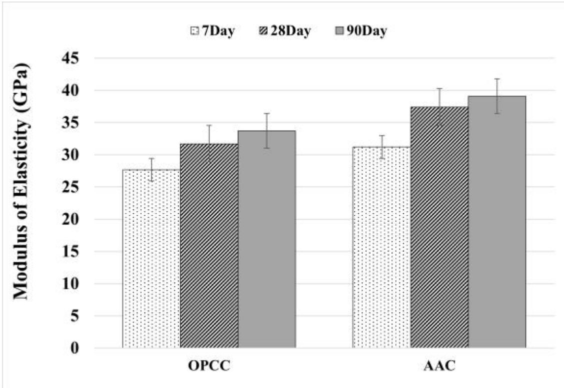

Figure 6. Results of the Modulus of Elasticity Test

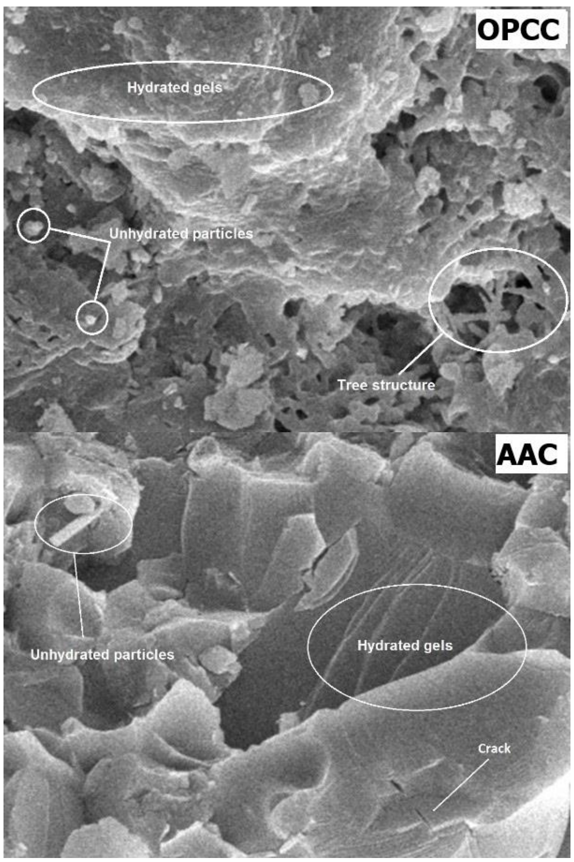

Figure 7. SEM Analysis Results

4. Conclusion

In this experimental study, the manufacture of AAC and its comparison with OPCC were investigated, following the tests of compressive strength, tensile strength and elastic modulus. SEM image analysis was also performed for microstructural evaluations and verification of the results of other tests. The results obtained in this study are presented as follows.

1- Increasing the curing age of concrete samples improved the test results. In this regard, in OPCC, the highest compressive strength, tensile strength and elastic modulus were obtained at a curing age of 90 days, respectively, at 64.92, 5.22 MPa and 33.73 GPa, which resulted in an improvement of 48.79, 89.13 and 21.85 percent compared to a curing age of 7 days, respectively. In AAC, the highest compressive strength, tensile strength and elastic modulus were obtained at a curing age of 90 days, with values of 72.33, 4.74 MPa and 39.11 GPa, respectively, which resulted in an improvement of 10.93, 60.67 and 25.35 percent compared to the 7-day curing age, respectively.

2- At a curing age of 7 and 28 days, the results of the tests in AAC were improved compared to OPCC. At a curing age of 90 days (as the optimal age), the performance of AAC in compressive strength, tensile strength and elastic modulus tests showed an improvement of 11.41 percent, a decrease of 19.9 percent and an improvement of 15.95 percent, respectively.

3- The results of the SEM image analysis on concrete samples overlapped and were consistent with other tests in this study.

Data Availability

The data used to support the findings of this study is available from the corresponding author upon request.

Conflicts of Interest

The authors declare that they have no conflicts of interest regarding the publication of this paper.

Funding

No funding was received.

Reference

Abd Elaty, M.A.A. (2014). Compressive strength prediction of Portland cement concrete with age using a new model. *HBRC Journal*, 10(2), 145-155.

Allahverdi, A. L. I., Kani, E. N., & Yazdanipour, M. (2011). Effects of blast-furnace slag on natural pozzolan-based geopolymer cement. *Ceramics-Silikáty*, 55(1), 68-78.

Davidovits, J. (2008). *Geopolymer chemistry and application* (2nd ed.). Institut Géopolymère, France.

Deb, P., Nath, P., & Sarker, P. (2015). Drying shrinkage of slag blended fly ash geopolymer concrete cured at room temperature. *Procedia Engineering*, 125, 594-600.

Duan, P., Shui, Z., Chen, W., & Shen, C. (2013). Enhancing microstructure and durability of concrete from ground granulated blast furnace slag and metakaolin as cement replacement materials. *Journal of Materials Research and Technology*, 2(1), 52-59.

Du, H., Du, S., & Liu, X. (2014). Durability performances of concrete with nano-silica. *Construction and Building Materials*, 73, 705-712.

Pirmohammadi Alishah, F., & Mahmoudzadeh, N. (2020). Investigation of the effect of bentonite paste index on modulus of elasticity, compressive strength and performance of plastic concrete. *Civil and Project*, 2(5), 87-109.

Ganesh, P., Ramachandra Murthy, A., Sundar Kumar, S., Mohammed Saffiq Reheman, M., & Iyer, N. R. (2016). Effect of nanosilica on durability and mechanical properties of high-strength concrete. *Magazine of Concrete Research*, 68(5), 229-236.

Hatami Zargaran, M. (2024). Examination of the Influence of Cut-off Wall Length on Uplift Forces in Diversion Dams (Case Study: Borj Dam). *Journal of Hydraulic and Water Engineering*, 2(1), 29-42. doi: 10.22044/jhwe.2024.14105.1033

Jorabloo, M., Sarbazi, N., & Aminian, P. (2024). Studying the Impact of Dam Construction on the Hydrologic Regime in the Garmsar Plain. *Journal of Hydraulic and Water Engineering*, 2(1), 1-12. doi: 10.22044/jhwe.2023.12568.1002

Kazemian, S., & Ghareh, S. (2017). Effects of Cement, Different Bentonite, and Aggregates on Plastic Concrete in Besh-Ghardash Dam, Iran. *Journal of Testing and Evaluation*, 45(1), 242-248.

Khalighi, F., Ahmadi, A., Keramat, A., & Tijsseling, A. (2024). A Hybrid Solution for Transient Pipe Flow based on Method of Characteristics and Lax-Friedrichs Scheme. *Journal of Hydraulic and Water Engineering*, 2(1), 13-28. doi: 10.22044/jhwe.2024.13086.1015

Kim, J.K., Moon, Y.H., & Eo, S.H. (1998). Compressive strength development of concrete with different curing time and temperature. *Cement and Concrete Research*, 28(12), 1761-1773.

Madandoust, R., Bungey, J.H., & Ghayidel, R. (2012). Prediction of the concrete compressive strength by means of core testing using GMDH-type neural network and ANFIS models. *Computational Materials Science*, 51(1), 261-272.

Mansourghanaei, M., Biklaryan, M., & Mardookhpour, A. (2024). Durability and mechanical properties of granulated blast furnace slag based geopolymer concrete containing polyolefin fibers and nano silica. *KSCE Journal of Civil Engineering*, 28(1), 209-219.

Mansourghanaei, M., Biklaryan, M., & Mardookhpour, A. (2023). Experimental study of properties of green concrete based on geopolymer materials under high temperature. *Civil Engineering Infrastructures Journal*, 56(2), 365-379.

Mansourghanaei, M., & Mardookhpour, A. (2024). Analysis of the Numerical Results Obtained from the Experimental Examination of the Mechanical Properties of Geopolymer Concrete. *Numerical Methods in Civil Engineering*, 9(1), 31-41.

Mansourghanaei, M., Biklaryan, M., & Mardookhpour, A. (2023). Experimental Study of Mechanical Properties of Slag Geopolymer Concrete under High Temperature, Used in Road Pavement. *International Journal of Transportation Engineering*, 11(1), 1371-1385.

Mehta, P. K., & Monteiro, P. J. (2014). *Concrete: microstructure, properties, and materials*. McGraw-Hill Education.

Naderi, M., Valibeigi, R., & Mirsafi, S. M. (2018). Studying the Effects kind of Curing on Strengths and Permeability of Concrete. *Journal of Structural and Construction Engineering*, 5(3), 106-123.

Neupane, N., Chalmers, D., & Kidd, P. (2018). High-strength geopolymer concrete—properties. advantages and challenges. *Advances in Materials*, 7(2), 15-25.

Nofallah, M. H. (2018). Effect of sodium Hydroxide solution concentration and sodium silicate to sodium hydroxide ratio on the compressive strength and water absorption of slag based alkali-activated concrete. *Concrete Research*, 11(2), 95-103.

Jafari Nadoushan, M., & Ramezanianpor, A. (2019). Mechanical Properties of Alkali Activated Slag Pastes and Determination of Optimum Values of Effective Factors. *Amirkabir Journal of Civil Engineering*, 50(6), 1043-1052. doi: 10.22060/ceej.2017.11113.4977

Nosrati, A., Zandi, Y., Shariati, M., Khademi, K., Aliabad, M., Marto, A., & Khorami, M. (2018). Portland cement structure and its major oxides and fineness. *Smart Structures and Systems*, 22(2), 425-432.

Nuaklong, P., Sata, V., & Chindaprasirt, P. (2016). Influence of recycled aggregate on fly ash geopolymer concrete properties. *Journal of Cleaner Production*, 112, 2300-2307.

Pilehvar, S., DuyCao, V., M.Szczotok, A., Carmona, M., Valentini, L., Lanzón, M., & LenaKjøniksen, A. (2018). Physical and mechanical properties of fly ash and slag geopolymer concrete containing different types of microencapsulated phase change materials. *Construction and Building Materials*, 173, 28-39.

Singh, B., Ishwarya, G., Gupta, M., & Bhattacharyya, S. K. (2015). Geopolymer concrete: A review of some recent developments. *Construction and Building Materials*, 85, 78-90.

Shirgir, B., ALIZADEH, G. H., & Shirgir, V. (2017). An experimental study on the abrasion resistance of pervious concrete containing nano SiO2 in pavement.

Vora, P., & Urmil V, D. (2013). Parametric studies on compressive strength of geopolymer concrete. *Procedia Engineering*, 51, 210-219.

Zhuang, X. Y., Chen, L., Komarneni, S., Zhou, C. H., Tong, D. S., Yang, H. M., ... & Wang, H. (2016). Fly ash-based geopolymer: clean production, properties and applications. *Journal of Cleaner Production*, 125, 253-267.